Organic Electronics 13 (2012) 1881–1886

Contents lists available at SciVerse ScienceDirect

Organic Electronics

journal homepage: www.elsevier.com/locate/orgel

Silver nanowire-polymer composite electrode for high performance solution-processed thin-film transistors

Liang-Hsiang Chen [a], Pang Lin [a], Ming-Chou Chen [b], Peng-Yi Huang [b], Choongik Kim [c,*], Jia-Chong Ho [d], Cheng-Chung Lee [d]

[a] Department of Materials Science and Engineering, National Chiao-Tung University, Hsinchu, Taiwan, ROC
[b] Department of Chemistry, National Central University, Chung-Li, Taiwan, ROC
[c] Department of Chemical and Biomolecular Engineering, Sogang University, 1 Shinsoo-Dong, Mapo-gu, Seoul 121-742, Republic of Korea
[d] Process Technology Division, Display Technology Center, Industrial Technology Research Institute, Hsinchu, Taiwan, ROC

ARTICLE INFO

Article history:
Received 25 March 2012
Received in revised form 4 May 2012
Accepted 12 May 2012
Available online 15 June 2012

Keywords:
Organic thin-film transistor (OTFT)
Conductive electrode
Silver nanowire
Anthradithiophene

ABSTRACT

Silver nanowires (AgNWs)/poly-(3,4-ethylenedioxythiophene/polystyrene sulphonate) (PEDOT:PSS) composite films as conductive electrode for OTFTs were prepared, and their optical and electrical properties were investigated. The conductive composite films used in this study afforded low sheet resistance of <140 Ω/sq and transmittance as high as 70% in the visible region. For the composite film with 0.1 wt.% of AgNWs, contact resistance as low as 2.7×10^4 Ω cm was obtained, as examined by Transfer length model (TLM) analysis, and work function of the corresponding film was 5.0 eV. Furthermore, the composite films were employed as source and drain electrodes for top-gate/bottom-contact organic thin-film transistors (OTFTs) based on solution-processed 5,11-bistriethylsilylethynyl anthradithiophene (TES-ADT) as organic semiconductor, and the resulting device showed high electrical performance with carrier mobility as high as 0.21 cm^2/ V s.

1. Introduction

Organic thin-film transistors (OTFTs) have extensively been studied for low cost, lightweight, flexible electronics such as smart cards, identification tags, active-matrix displays, and sensors [1]. Hence, the development of solution-processed components — semiconductors, insulators, and conductors — in OTFTs at low cost and in a large scale, are of great interest [2]. There have been great efforts to develop and improve the electrical properties of solution-processed organic semiconductors, some of which perform comparably to amorphous silicon [3,4]. Furthermore, polymers or polymer-based composite films with high capacitance and low leakage current density have been investigated as high performance solution-processed insulators [5]. Solution-processed conductors, however, have received relatively little attention, despite their critical roles in OTFTs. The high performance conductor materials need to meet several electrical and material requirements – (i) high electrical conductivity, (ii) proper energy match with organic semiconductor, and (iii) processibility at low temperature that is compatible with flexible substrates.

Conductive materials that have mostly been employed in OTFTs are metals such as gold, due to their high conductivity. However, physical damage onto the underlying organic layers caused by vacuum deposition could deteriorate the device performance. Solution-processed conductive materials such as poly-(3,4-ethylenedioxythiophene/polystyrene sulphonate) (PEDOT:PSS) and doped polyaniline have been employed in OTFTs, but they suffer from low electrical conductivity [6]. Recently, other candidates for conductive materials such as carbon nanotubes, metal grids, and metallic nanowires have also been investigated [7]. Among them, random silver nanowire (AgNW)

* Corresponding author.
E-mail address: choongik@sogang.ac.kr (C. Kim).

1566-1199/$ - see front matter © 2012 Elsevier B.V. All rights reserved.
http://dx.doi.org/10.1016/j.orgel.2012.05.040

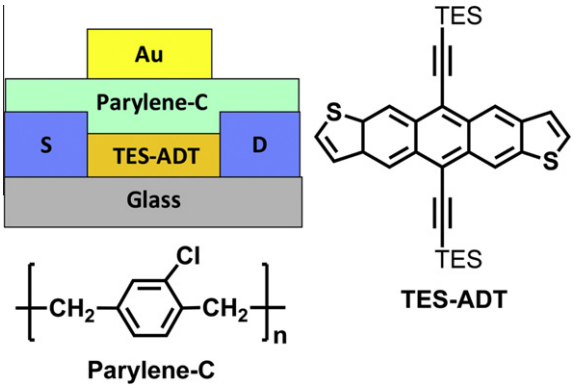

Fig. 1. Top-gate/bottom-contact TFT structure, and chemical structures of TES-ADT and Parylene-C employed in this study.

networks are promising candidates because of their attractive electrical, thermal, and optical properties [8]. Although AgNW-based conductive films found some applications in electronic devices, these films have never been employed in solution-processed OTFTs, to the best of our knowledge [8]. To this end, we report conductive composite films based on AgNW and PEDOT:PSS with varying AgNW contents, and their electrical, optical, and material properties in terms of sheet resistance (R_s), contact resistance (R_c), work function, and optical transparency were investigated. Furthermore, the potential of AgNW-based composite conductors for electronic devices was evaluated for top-gate/bottom-contact OTFTs by employing composite conductors as source/drain contacts, 5,11-bistriethylsilylethynyl anthradithiophene (TES-ADT) [4,9], a representative high performance solution-processed p-type organic material, as semiconductors, and Parylene C as gate insulator (Fig. 1).

2. Experimental section

2.1. Materials

All chemicals were purchased from Aldrich, including the PEDOT:PSS (1.3 wt.% dispersion in H_2O), and were used without further purification. AgNWs were prepared using a synthetic procedure in the literature [10,11]. Organic semiconductor, TES-ADT, was synthesized following the synthetic procedure in the literature [4], and the synthetic product was purified further by chromatography (silica gel) and recrystallization.

2.2. Preparation and characterization of AgNW-PEDOT:PSS composite films

For composite conductive films, a desired amount of AgNWs stabilized with trisodium citrate in water (0.1 wt.%, 0.5 wt.%, and 1 wt.%) was added to the PEDOT:PSS solution (10 mL). For pristine AgNW films (0.1 wt.%, without PEDOT:PSS), deionized water (10 mL) was used instead of PEDOT:PSS solution. The solution was sonicated for 30 min using a high intensity ultrasonic probe to prevent local inhomogeneity before spin-coating.

To form the composite films, the mixtures (AgNWs and PEDOT:PSS) were spin-coated (1500 rpm) on a glass substrate, and the resulting films were annealed at 100, 150, 200, and 250 °C for 2 h on a hotplate. The thickness of the composite films was ~500 nm, as estimated via a Dektak 3030 profilometer. The sheet resistances of the composite films were measured using a 4-point probe technique (Keithley 2400 source meter). Optical transmittance of the films were measured on quartz slides from 300 nm to 800 nm (with an increment of 5 nm) using a Perkin–Elmer Lambda 750 UV/Vis/NIR spectrophotometer. The surface morphologies of the films were analyzed using atomic force microscopy (AFM, Digital Instruments Nanoscope III) and scanning electron microscopy (SEM, Hitachi S-4700). The work function of the films was analyzed by ultraviolet photoemission spectroscopy (UPS) with line source energy of He I (21.21 eV).

2.3. Device fabrication and characterization

To fabricate the top-gate/bottom-contact OTFT, conductive composite films on glass substrates were patterned as source/drain contacts, by focused laser ablation using a UV laser beam (λ = 365 nm). The channel width of the resulting electrodes was 500 μm, and the channel lengths were 20 μm, 30 μm, 40 μm, and 50 μm (various channel lengths were employed to extract the contact resistances of the devices). Organic semiconductor (TES-ADT) was spin-coated onto the substrates from a 20 mL toluene solution (1 wt.%) at 500 rpm for 2 s and 1000 rpm for 28 s. The resulting film was thermally annealed at 90 °C for 2 min in a N_2 glove box. The film thickness of the semiconducting film was ~90 nm, as measured by AFM. To improve the crystallinity of the active layer, TES-ADT films were annealed under chloroform solvent-vapor (at a vapor pressure of 12 kPa) for 5 min in a glass chamber. For an insulating layer, Parylene-C was deposited by vapor phase polymerization system (chemical vapor polymerization reactor consisted of a vaporizer, pyrolysis and polymerization chambers, a cold trap, and a vacuum system) [12]. The film thickness of the insulator was ~900 nm with an areal capacitance value of 2.7 nF/cm^2. For gate electrode, a 50 nm-thick Au layer was thermally evaporated through a shadow mask. The electrical characteristics of the devices were measured under darkness with a semiconductor parameter analyzer (HP 4155A) at room temperature in a glove box (H_2O < 10 ppm).

3. Results and discussion

To investigate the electrical conductivity of the AgNW-PEDOT:PSS composite films in comparison to that of pristine PEDOT:PSS film and random AgNW networks (pristine AgNW films), sheet resistances (Ω/sq) of the films were measured as a function of film annealing temperature (Fig. 2A). In general, sheet resistances of the measured films gradually decreased as the annealing temperature increased, then reached a nearly constant values at annealing temperature >200 °C. Furthermore, sheet resistances of the composite films, regardless of the AgNW contents, were

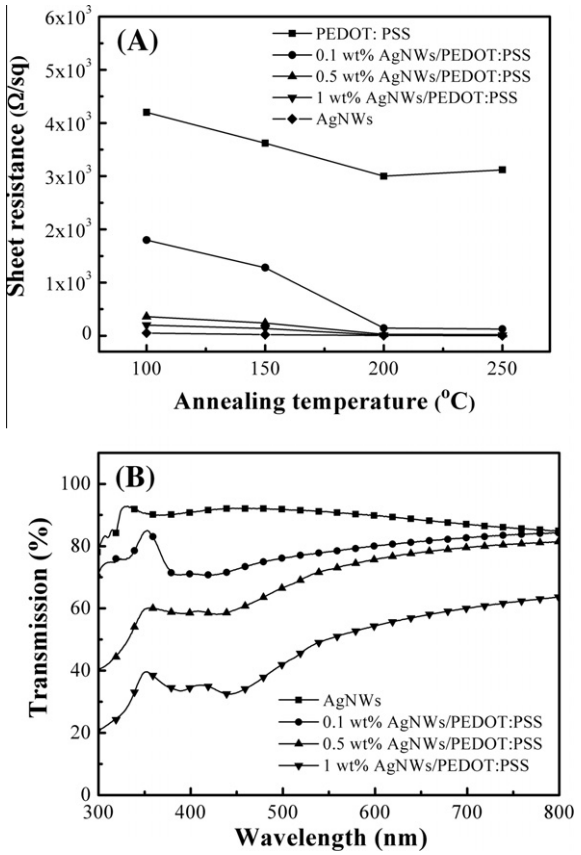

Fig. 2. (A) Sheet resistances of the conductive composite films as a function of annealing temperature. (B) Optical transmittance spectra of the conductive films on glass substrates.

much lower than that of pristine PEDOT:PSS film. For example, at annealing temperature of 200 °C, sheet resistance of the PEDOT:PSS film was $\sim 3 \times 10^3$ Ω/sq, while the composite films exhibited higher electrical conductivity with sheet resistance values of 9–140 Ω/sq, comparable to that of AgNW film (5 Ω/sq) at the same annealing temperature. High electrical conductivity of the composite films achieved at relatively low annealing temperature could be attributed to the formation of a 3D conductive network via random AgNW networks in polymer matrices (vide infra, Fig. S1), which shows the promise of the present composite films used on plastic substrates for flexible electronics.

Optical properties of the composite films with varying AgNW contents were investigated by UV–Vis spectroscopy [13]. Fig. 2B shows optical transmittance spectra of the conductive films on glass substrates at a range of 300–800 nm. As shown, optical transparency of the conductive composite films were lower than that of pristine AgNW films. Average optical transmittance of the pristine AgNW films were ~86% in the measured region, comparable to that of AgNW films reported as transparent conductors in the literatures [14,15]. Furthermore, as the content of AgNWs increased in the composite films, the optical transparency decreased. The average optical transmittance of the conductive composite films with 0.1 wt.%, 0.5 wt.%, and 1 wt.% of AgNW contents were 70%, 62%, and 45%, respectively [16]. Low optical transparency of the composite films with high AgNW contents might be attributed to the formation of AgNW aggregates, which could deteriorate optical properties of the films (Fig. S1) [17].

To test the potential of the conductive composite films for electronic devices, top-gate/bottom-contact OTFTs were fabricated by employing the composite films as source/drain contacts, TES-ADT as organic semiconductor, and Parylene-C as organic insulator (Fig. 1). Fig. 3 and Table 1 collect the typical TES-ADT TFT characteristics with varying AgNW contents. Note that the saturation mobility (μ_{sat}) and the threshold voltage (V_T), an average value of ten device measurements, were calculated at $V_{DS} = -50$ V. Overall, TES-ADT TFTs employing the composite films as conductors showed much higher device performance (carrier mobility of 0.03–0.21 cm^2/V s) compared to the device with pristine AgNW films as contacts (carrier mobility of 0.008 cm^2/V s). Especially, the TES-ADT TFTs constructed with 0.1 wt.% AgNW-PEDOT:PSS composite films showed highest electrical performance with carrier mobility as high as 0.21 ± 0.05 cm^2/V s, demonstrating the promise of the conductive composite films as conductors for OTFTs. Figs. 3B and S2 show output characteristics of the TES-ADT TFTs with 0.1 wt.% AgNW-PEDOT:PSS composite film and pristine AgNW film as conductors, respectively. The TFT with electrodes of 0.1 wt.% AgNW-PEDOT:PSS composite films exhibited relatively reasonable output characteristics with pinch-off and current saturation behaviors (Fig. 3B). On the other hand, the TFT with electrodes of pristine AgNW films showed more current crowding in the low drain voltage region (linear region) compared to that with electrodes of composite films, which could be attributed to the high contact resistance between the AgNW electrodes and the TES-ADT channel layer (Fig. S2, vide infra).

It has been reported that the performance of TES-ADT TFTs is highly dependent upon the manner in which electrical contacts are made to the organic semiconductors, due to weak van der Waals interactions between TES-ADT molecules in the solid state [18]. For example, TES-ADT TFTs employing laminated gold source/drain electrodes via elastomeric stamps showed higher device performance compared to those with gold electrodes fabricated via thermal evaporation [18]. To investigate the nature of the electrical contacts between electrodes and TES-ADT active layer, contact resistances and work functions of the conductive films were examined.

First, for contact resistance calculation, TLM analysis was used, in which the total resistance (R_{tot}) of a device was fitted as a function of the channel length (L) [19,20]. Then, the contact resistance (R_c) was obtained at the intersection of the measured device resistance in the limit of $L \rightarrow 0$ at different gate voltage (V_G), as indicated by Eq. 1:

$$R_{tot} = R_c + \frac{L}{W[\mu C_i(V_G - V_{th})]} \quad (1)$$

where μ and V_T are the intrinsic field-effect mobility and the threshold voltage, respectively. Fig. 4A shows R_{tot} of TES-ADT TFTs with pristine AgNW films as contacts,

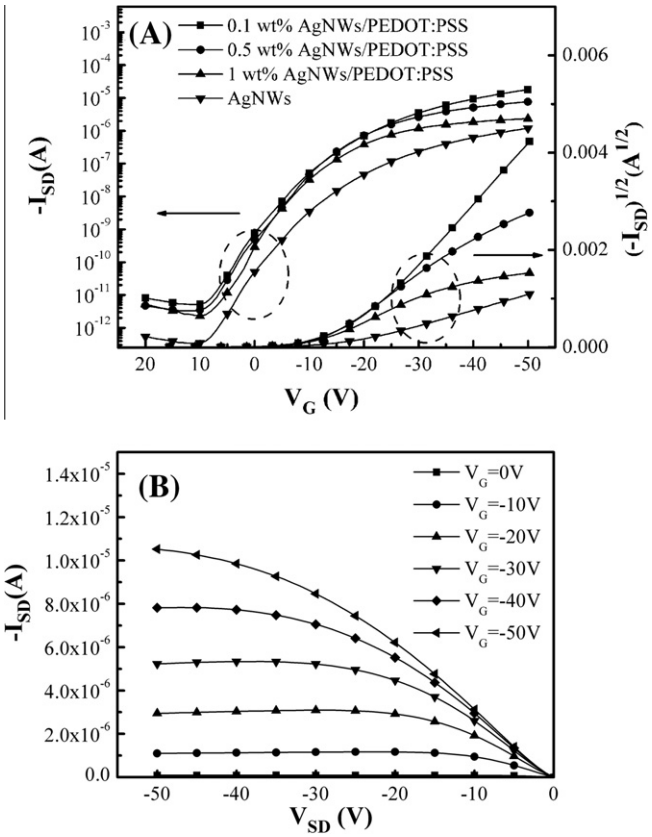

Fig. 3. Electrical characteristics of top-gate/bottom-contact TES-ADT TFTs. (A) Transfer characteristics of TFTs employing the conductive composite films (with varying AgNW contents) and pristine AgNW films as source/drain contacts. (B) Output characteristics of TFTs employing the 0.1 wt.% AgNW-PEDOT:PSS composite films as source/drain contacts.

Table 1
Charge carrier mobility (μ_{sat}, $cm^2/V\,s$), current on/off ratios (I_{on}/I_{off}), threshold voltage (V_T, V), subthreshold swing (*S.S.*, V/decade), and contact resistance (R_c, $M\Omega\,cm$) data for TES-ADT TFTs fabricated with pristine AgNW films and AgNW-PEDOT:PSS composite films with varying AgNW contents as source/drain contacts.

Samples	μ_{sat}	I_{on}/I_{off}	V_T	*S.S.*	R_c
AgNWs	0.008 ± 0.005	5.0×10^5	−15 ± 5.0	1.5 ± 0.8	5.4 ± 2.1
1 wt.% AgNWs/PEDOT:PSS	0.03 ± 0.02	1.5×10^6	−7.0 ± 4.0	1.4 ± 0.6	1.5 ± 0.8
0.5 wt.% AgNWs/PEDOT:PSS	0.15 ± 0.03	3.0×10^6	−10 ± 3.0	1.2 ± 0.3	0.067 ± 0.023
0.1 wt.% AgNWs/PEDOT:PSS	0.21 ± 0.05	5.0×10^6	−8.0 ± 2.0	1.3 ± 0.5	0.027 ± 0.012

normalized by the channel width, plotted as a function of channel length L at different V_G. The obtained contact resistances of the conductive films employed in this study at different gate voltage are shown in Fig. 4B. As shown, contact resistances normalized with the channel width ($R_c \cdot W$), of the films decreased as the gate voltage increased, in consistent with the previous study in the literature [21]. For example, contact resistances of the pristine AgNW films were $2.0 \times 10^8\,\Omega\,cm$ and $5.4 \times 10^6\,\Omega\,cm$ at a gate voltage of −10 V and −50 V, respectively. Furthermore, the conductive composite films employed in this study afforded much lower contact resistances than pristine AgNW films. For AgNW-PEDOT:PSS composite films with 0.1 wt.%, 0.5 wt.%, and 1 wt.% of AgNW contents, the corresponding contact resistances at a gate voltage of −50 V were $2.7 \times 10^4\,\Omega\,cm$, $6.7 \times 10^4\,\Omega\,cm$, and $1.5 \times 10^6\,\Omega\,cm$, respectively. Higher contact resistances of the composite films with larger contents of AgNWs might be due to defected semiconductor–electrode interface originated from large surface roughnesses (Fig. S1) [17,22].

Secondly, work functions of the conductive films were determined by ultraviolet photoemission spectra (UPS, He(I): 21.2 eV), via calculation of the UPS spectra width (Fig. 5). Measured work functions of the pristine AgNW film was ~4.2 eV, while those of AgNW-PEDOT:PSS composite films with 0.1 wt.%, 0.5 wt.%, and 1 wt.% of AgNW contents were 5.0 eV, 4.8 eV, and 4.5 eV, respectively. Work functions of the conductive composite films decreased as the contents of AgNWs in the film increased. The lowest contact resistance and highest work function of

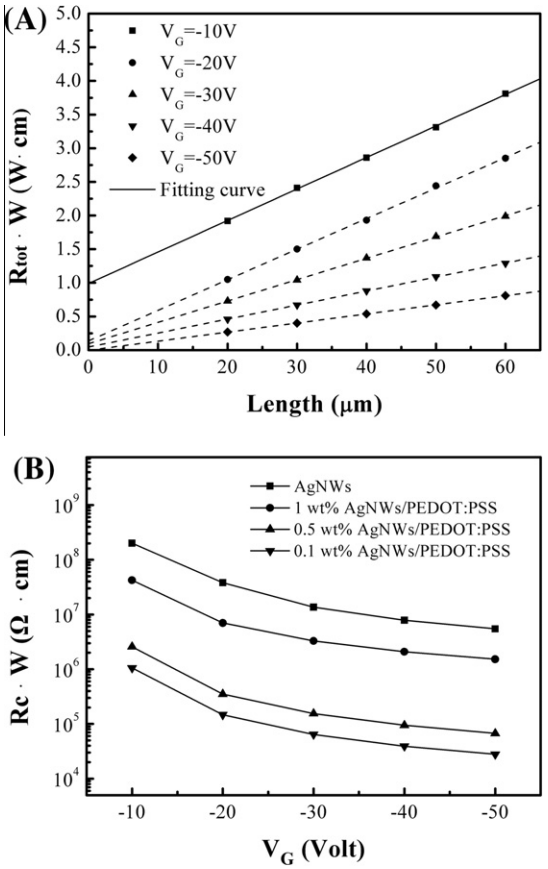

Fig. 4. (A) Total normalized resistances as a function of channel length for TES-ADT TFTs with pristine Ag NW films as source/drain electrodes at various V_G. (B) Contact resistances of the conductive films employed in this study as a function of gate voltage, normalized with the channel width.

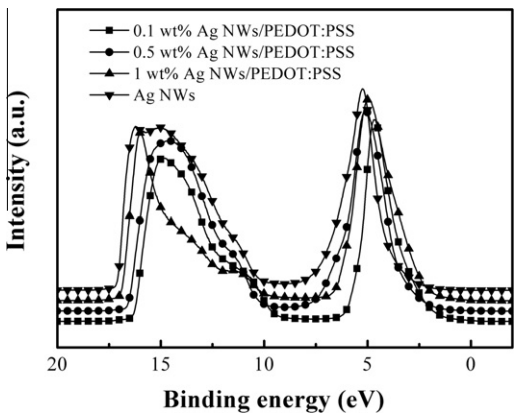

Fig. 5. UPS spectra of the conductive films employed in this study.

the 0.1 wt.% AgNW-PEDOT:PSS composite film could afford better energy level match with better charge carrier injection into the active layer, resulting in better device performance (vide supra) [23].

4. Conclusions

This study reported TES-ADT TFTs using spin-coated conductive composite films based on AgNWs and PEDOT:PSS as source and drain electrodes. The composite films with low content of AgNW (0.1 wt.%) showed low sheet resistance of 140 Ω/sq and decent optical transmittance of 70%. Furthermore, low contact resistance and high work function of the corresponding composite film afforded good electrical contacts and energy-level alignment to an active layer, resulting in high performance top-gate/bottom-contact TES-ADT TFTs with carrier mobility up to 0.21 cm^2/V s. These results demonstrated the viability of using spin-coated conductive composite films as source and drain electrodes for large area and flexible electronic applications.

Acknowledgements

This work was supported by the Display Technology Center for the Industrial Technology Research Institute of Taiwan, R.O.C. (Contract No. B301AR1L11), by National Science Council, Taiwan, Republic of China (Grant Nos. NSC100-2628-M-008-004 and NSC100-2627-E-006-001), and by the National Research Foundation of Korea (2011-0007730), and by a Grant (2011-0031628) from the Center for Advanced Soft Electronics under the Global Frontier Research Program of the Ministry of Education, Science and Technology, Korea.

Appendix A. Supplementary data

Supplementary data associated with this article can be found, in the online version, at http://dx.doi.org/10.1016/j.orgel.2012.05.040.

References

[1] 1a C.D. Dimitrakopoulos, P.R.L. Malenfant, Adv. Mater. 14 (2002) 99;
1b B. Crone, A. Dodabalapur, Y.Y. Lin, R.W. Filas, Z. Bao, A. LaDuca, R. Sarpeshkar, H.E. Katz, W. Li, Nature 403 (2000) 521;
1c Y.Y. Lin, D.J. Gundlach, S.F. Nelson, T.N. Jackson, IEEE Electron Device Lett. 18 (1997) 606.

[2] 2a C.D. Sheraw, T.N. Jackson, D.L. Eaton, J.E. Anthony, Adv. Mater. 15 (2003) 2009;
2b H. Usta, A. Facchetti, T.J. Marks, Acc. Chem. Res. 44 (2011) 501;
2c J. Youn, M.-C. Chen, Y.-J. Liang, H. Huang, R.P. Ortiz, C. Kim, C. Stern, T.-S. Hu, L.-H. Chen, J.-Y. Yan, A. Facchetti, T.J. Marks, Chem. Mater. 22 (2010) 5031;
2d J. Youn, P.-Y. Huang, Y.-W. Huang, M.-C. Chen, Y.-J. Lin, H, Huang, R. P. Ortiz, C. Stern, M.-C. Chung, C.-Y. Feng, A. Facchetti, T. J. Marks, Adv. Funct. Mater. 22 (2012) 48;
2e M.-C. Chen, C. Kim, S.-Y. Chen, Y.-J. Chiang, M.-C. Chung, A. Facchetti, T.J. Marks, J. Mater. Chem. 18 (2008) 1029.

[3] 3a W.H. Lee, D.H. Kim, Y. Jang, J.H. Cho, M. Hwang, Y.D. Park, Appl. Phys. Lett. 90 (2007) 132106;
3b J.G. Laquindanum, H.E. Katz, A.J. Lovinger, J. Am. Chem. Soc. 120 (1998) 664;
3c M.M. Payne, S.A. Odom, S.R. Parkin, J.E. Anthony, Org. Lett. 6 (2004) 3325;
3d C. Kim, P.Y. Huang, J.W. Jhuang, M.C. Chen, J.Y. Ho, L.H. Chen, G.H. Lee, A. Facchetti, T.J. Marks, Org. Electron. 11 (2010) 1363;
3e P.-Y. Huang, C. Kim, M.-C. Chen, Synlett 15 (2011) 2151.

[4] M.M. Payne, S.R. Parkin, J.E. Anthony, C. Kuo, T.N. Jackson, J. Am. Chem. Soc. 127 (2005) 4986.

[5] 5a R.P. Ortiz, A. Facchetti, T.J. Marks, Chem. Rev. 110 (2010) 205;
5b A. Facchetti, M.-H. Yoon, T.J. Marks, Adv. Mater. 17 (2005) 1705.

[6] 6a K. Fehse, K. Walzer, K. Leo, W. Lovenich, A. Elschner, Adv. Mater. 19 (2007) 441;
6b P.G. Taylow, J.-K. Lee, A.A. Zakhidov, M. chatzichristidi, H. H. Fong, J. A. DeFranco, G. G. Malliaras, C. K. Ober, Adv. Mater. 21 (2009) 2314.
[7] 7a H. Gu, T.M. Swager, Adv. Mater. 20 (2008) 4433;
7b J.H. Lee, D.W. Shin, V.G. Makotchenko, A.S. Nazarov, V.E. Fedorov, Y.-H. Kim, J.-Y. Choi, J.M. Kim, J.-B. Yoo, Adv. Mater. 21 (2009) 4383;
7c M.-G. Kang, M.-S. Kim, J. Kim, L.J. Guo, Adv. Mater. 20 (2008) 4408;
7d S. De, T.M. Higgins, P.E. Lyons, E.M. Doherty, P.N. Nirmalraj, W.J. Blau, J.J. Boland, J.N. Coleman, ACS Nano 3 (2009) 1767;
7e F. Cicoira, C.M. Aguirre, R. Martel, ACS Nano 5 (2011) 283;
7f F. Cicoira, N. Coppede, S. Iannotta, R. Martel, Appl. Phys. Lett. 98 (2011) 183303.
[8] 8a Y. Sun, Nanoscale 2 (2010) 1626;
8b J.-Y. Lee, S.T. Connor, Y. Cui, P. Peumans, Nano Lett. 8 (2008) 689;
8c L. Hu, H.S. Kim, J.-Y. Lee, P. Peumans, Y. Cui, ACS Nano 4 (2010) 2955.
[9] K.C. Dickey, J.E. Anthony, Y.L. Loo, Adv. Mater. 18 (2006) 1721.
[10] Y. Sun, Y. Yin, B.T. Mayers, T. Herricks, Y. Xia, Chem. Mater. 14 (2002) 4736.
[11] The length and width of AgNWs were 16–20 μm and 100–120 nm, respectively.
[12] C.R. Newman, R.J. Chesterfield, M.J. Panzer, C.D. Frisbie, J. Appl. Phys. 98 (2005) 084506.
[13] Optical transparency is an important property for other applications such as light-emitting diodes and photovoltaics.
[14] L. Yang, T. Zhang, H. Zhou, S.C. Price, B.J. Wiley, W. You, Appl. Mater. Interf. 3 (2011) 4075.
[15] L. Hu, H.S. Kim, J.Y. Lee, P. Peumans, Y. Cui, Nano Lett. 4 (2010) 2955.
[16] The composite film with lowest AgNW content (0.1 wt.%) showed decent transparency, which could potentially be useful for a variety of applications which require transparent conductors.
[17] Surface morphologies of the composite films, as measured by AFM and SEM, showed AgNW aggregates, especially for composite films with high contents of AgNWs. The root-mean-square (RMS) roughnesses of the composite films with AgNW contents of 0.1 wt.%, 0.5 wt.%, and 1 wt.% were 1.5 nm, 8.5 nm, and 12.5 nm, respectively.
[18] K.C. Dickey, T.J. Smith, K.J. Stevenson, S. Subramanian, J.E. Anthony, Y.-L. Loo, Chem. Mater. 19 (2007) 5210.
[19] W.S. Kim, Y.K. Moon, K.T. Kim, J.H. Lee, B.D. Ahn, J.W. Park, Thin Solid Films 518 (2010) 6357.
[20] TLM analysis was performed at VDS of 0 to −1 V, at which the linear behavior is clear.
[21] J. Li, L. Zhang, X.W. Zhang, H. Zhang, X.Y. Jiang, D.B. Yu, W.Q. Zhu, Z.L. Zhang, Curr. Appl. Phys. 10 (2010) 1302.
[22] V. Sholin, S.A. Carter, R.A. Street, A.C. Arias, Appl. Phys. Lett. 92 (2008) 063307.
[23] The HOMO level of TES-ADT is ∼5.1 eV, whose energy level matches well with the work function of the 0.1 wt.% AgNW-PEDOTPSS composite film.